A Unified Framework for Posing Strongly-Coupled Multiphysics for Robotics Simulation

Jeong Hun Lee
Robotics Institute
Carnegie Mellon University
jeonghunlee@cmu.edu

Junzhe Hu
Robotics Institute
Carnegie Mellon University
junzhehu@andrew.cmu.edu

Sofia Kwok
Robotics Institute
Carnegie Mellon University
sofiak@andrew.cmu.edu

Carmel Majidi
Robotics Institute
Carnegie Mellon University
carmel.majidi@cmu.edu

Zachary Manchester
Robotics Institute
Carnegie Mellon University
zacm@cmu.edu

Abstract: We present a framework for posing multiphysics as a single, unified optimization problem for downstream robotics simulation. Specifically, we apply our framework to the fluid-robot interaction setting, where the governing coupled manipulator and incompressible Navier-Stokes equations are derived together from a single Lagrangian using the principal of least action. We then employ discrete variational mechanics to derive a stable, implicit time-integration scheme for jointly simulating both the fluid and robot dynamics, which are tightly coupled by a constraint that enforces the no-slip boundary condition at the fluid-robot interface. We demonstrate our approach's physical accuracy on a novel swimming robot in simulation and validate results on real-world hardware, showcasing our framework's sim-to-real capability. In future work, we hope to extend our unified framework to pose other multiphysics settings commonly found in robotics, such as the manipulation of deformable objects.

Keywords: Multiphysics, Non-Rigid Simulation, Robotics

1 Introduction

In recent years, there has been considerable interest in designing robot control policies in multiphysics settings such as deformable-object manipulation [1, 2, 3], fluid transport [4, 5], and locomotion [6, 7, 8]. However, real-world data collection and training in such complex environments presents a major challenge. As a result, multiphysics-simulation platforms [9, 10] have seen growing interest and ongoing development, with many robotics applications still lacking viable physics engines. One such application is bio-inspired locomotion for aquatic vehicles [11, 12, 13, 14, 15, 16, 17], where current robotics simulators are unable to simulate complex boundary conditions (e.g., free stream) and become intractable when the fluid must be modeled as a continuum. In addition, coupling the partial differential equations governing the fluids with the ordinary differential equations of rigid-body dynamics can be conceptually difficult.

Therefore, we propose a unified framework for jointly deriving and simulating fluid-robot multiphysics. Specifically, we formulate the combined Lagrangian using the principle of least action to model the multiphysics as a single continuous-time optimization problem. We apply this to the fluid-robot interaction setting, for which we derive the coupled incompressible Navier-Stokes and manipulator equations governing the fluid and robot dynamics, respectively, as depicted in Figure 1. We show that the multiphysics coupling stems from a constraint that enforces the no-slip boundary condition at the fluid-robot interface. We then employ discrete variational mechanics [18] to discretize the unified action directly, which results in an implicit time-integration scheme that naturally simulates the robot and fluid dynamics in a stable, coupled manner. We showcase our approach's

9th Conference on Robot Learning (CoRL 2025), Seoul, Korea.

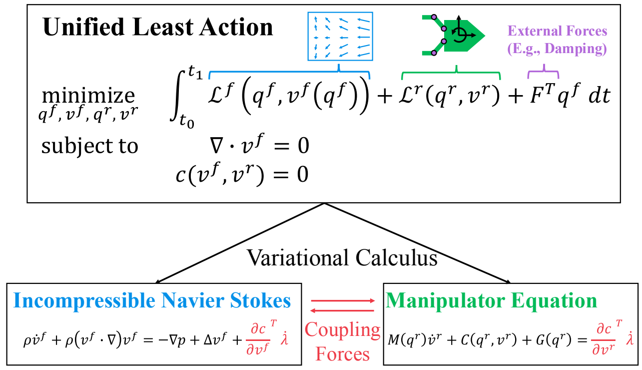

Figure 1: An overview of our multiphysics model, in which the unified Lagrangian governing the coupled fluid-robot dynamics is formulated using the principle of least action. Rather than the individual differential equations, the combined action is discretized directly to achieve tightly-coupled simulation.

ability to model an actuated robotic system, specifically a novel squid-inspired robot. We validate our simulation results on real-world hardware, showcasing the sim-to-real capabilities of our framework. In summary, our contributions are:

- A unified representation for strongly-coupled fluid-robot multiphysics via the principle of least action.
- An extension of variational integration for simulating multiphysics in the full state space of a robot.
- Demonstration of our approach in simulation with hardware validation on a bioinspired swimming robot.

The remainder of this paper is organized as follows: In Section 2, we describe our proposed approach for posing and simulating strongly-coupled multiphysics for the fluid-robot setting. In Section 3, we showcase the sim-to-real-transfer capabilities of our framework on a novel, squid-like swimming robot. In Section 4 we provide final concluding remarks and discuss future work.

2 METHODOLOGY

2.1 Fluid-Robot Multiphysics as Optimization

Existing simulators [9, 10] typically integrate over the individual differential equations before coupling the physics via explicit forces. As shown in Figure 1, we propose the least-action principle as an alternative, unified perspective of multiphysics from which the differential equations are derived. We refer the reader to comprehensive existing literature on variational principles for more details [18, 19, 20].

We begin by proposing the least-action principle for the combined multiphysics problem between a rigid (multi)body robot and an incompressible, Newtonian fluid (e.g., water):

$$\begin{aligned}
\underset{q_k^r, q^f, v^r, v^f}{\text{minimize}} \quad & \int_{t_0}^{t_f} L^f(q^f, v^f) + L^r(q^r, v^r) + F(t)^T q^f \, dt \\
\text{subject to} \quad & c_1(v^f) = \dot{q}^f - v^f(q^f) = 0 \quad \forall q^f \in \Omega, \\
& c_2(v^f) = \nabla \cdot v^f = 0 \quad \forall q^f \in \Omega, \\
& c_3(v^f) = v^f - v_{bc} = 0 \quad \forall q^f \in \partial\Omega, \\
& c_4(v^r) = \dot{q}^r - v^r = 0 \quad \forall q^r, \\
& c_5(q^r) = 0 \quad \forall q^r, \\
& c_6(v^f, v^r) = v^f - v^r = 0. \quad \forall q^f \in \Gamma
\end{aligned} \tag{1}$$

where Ω, Γ represent the fluid domain and robot geometry respectively with corresponding boundaries, $\partial\Omega, \partial\Gamma$; q^r, q^f are the configurations of the robot and fluid particle respectively and v^r, v^f are the corresponding velocities; $F(t) \in \mathbb{R}^n$ represents external forces such as damping. $c_1(v^f)$ encodes the kinematics constraint for the fluid-velocity field (i.e., an array of velocity sensors). $c_2(v^f)$ encodes the conservation-of-mass constraint while $c_3(v^f)$ enforces boundary conditions, v_{bc}, along the fluid-domain boundary (e.g., walls, free-stream velocity, etc.). $c_4(q^r)$ encodes the kinematics constraint of the robot while c_5 enforces other robot-configuration constraints, such as joint constraints found in manipulator arms. $c_6(v^f, q^r, v^r)$ encodes the no-slip constraint, which couples the robot and fluid physics by preventing the fluid from "penetrating" the robot boundary.

We first define the fluid and (single) rigid-body Lagrangians:

$$L^f(q^f, v^f) = \int_\Omega \tfrac{1}{2}\rho(v^f)^T v^f - \rho g^T q^f \, dV, \tag{2}$$

$$L^r(q^r, v^r) = \tfrac{1}{2}(v^r)^T M^r v^r - M^r g^T q^r, \tag{3}$$

where ρ is the fluid density; M is the mass matrix of the robot body; dV denotes the volume differential; and g is gravity. In this problem, damping is introduced by the fluid viscosity:

$$F(t) = \int_\Omega \mu \Delta v^f \, dV, \tag{4}$$

where μ is the dynamic viscosity of the fluid.

The first-order necessary (FON) conditions of (1) can be expressed by the variations w.r.t. q^r, v^r and q^f, v^f, which results in the coupled incompressible Navier-Stokes and manipulator equations, respectively:

$$\rho(\dot{v}^f + (v^f \cdot \nabla)v^f) = -\nabla p + \mu\nabla^2 v^f - \rho g - \frac{\partial c_3}{\partial v^f}^T \dot{\lambda}_3 - \frac{\partial c_6}{\partial v^f}^T \dot{\lambda}_6, \tag{5}$$

$$\nabla \cdot v^f = 0, \tag{6}$$

$$M\dot{v^r} + \rho g = \frac{\partial c_5}{\partial q^r}^T \lambda_5 - \frac{\partial c_6}{\partial v^r}^T \dot{\lambda}_6. \tag{7}$$

$$\dot{q}^r = v^r, \tag{8}$$

where $p = \dot{\lambda}_2 \in R^m$ is the fluidic pressure, which Lagrange [21] originally realized as the dual variable that enforces the conservation of mass. In similar fashion, the multiphysics-coupling force also corresponds to the no-slip-constraint Jacobian and the respective dual variable, $\dot{\lambda}_6$.

2.2 Coupled Discretization of the Fluid-Robot Multiphysics

Using the unified least-action principle of (1), we develop a variational integrator [18] to simulate fluid-robot multiphysics. First, we discretize the fluid domain spatially using a second-order finite-volume method [22], which provides a discrete counterpart to the following continuous operators:

$$\int_\Omega \rho v^f \, dV \Rightarrow M^f v^f, \qquad \int_\Omega \nabla p \, dV \Rightarrow Gp,$$

$$\int_\Omega (v^f \cdot \nabla) v^f \, dV \Rightarrow N(v^f), \qquad \int_\Omega \Delta v^f \, dV \Rightarrow L v^f.$$

Through a slight abuse of notation, we will use q^f, v^f, and p to refer to their discrete versions throughout the rest of this section. We may now express the spatially discrete fluid Lagrangian as:

$$L^f(q^f, v^f) = \tfrac{1}{2}(v^f)^T M^f v^f - M^f g^T q^f \, dV, \tag{9}$$

Using a midpoint quadrature rule, we then formulate the following discretized action:

$$
\begin{aligned}
\underset{q_k^r,\, q_k^f}{\text{minimize}} \quad & \sum_{k=1}^{2} L_d^f(q_k^f, q_{k+1}^f) + L_d^r(q_k^r, q_{k+1}^r) + \tfrac{h}{2} F(t_k + \tfrac{h}{2})^T (q_k^f + q_{k+1}^f) \\
\text{subject to} \quad & c_2(\bar{v}_k^f) = G^T \bar{v}_k^f = 0, \\
& c_3(\bar{v}_k^f) = B\bar{v}_k^f - v_{bc} = 0, \\
& c_5(\bar{q}_k^r) = 0, \\
& c_6(\bar{v}_k^f, \bar{v}_k^r) = 0,
\end{aligned}
\tag{10}
$$

where $\bar{q}_k$ and $\bar{v}_k$ are the configurations and velocities defined at the midpoint between t_k and t_{k-1}, $B\bar{v}_k^f$ extracts fluid velocities located at the fluid-domain boundary, and $c_6(\bar{v}^f, \bar{v}^r)$ is expressed using the immersed boundary method [23, 24]. $L_d(q_k, q_{k+1}) \in \mathbb{R}+$ is the discrete Lagrangian, which is expressed as:

$$
L_d(q_k, q_{k+1}) = hL(\underbrace{\tfrac{q_k + q_{k+1}}{2}}_{\bar{q}_{k+1}}, \underbrace{\tfrac{q_{k+1} - q_k}{h}}_{\bar{v}_{k+1}}). \tag{11}
$$

The external force is additionally modified to account for the convective term, $N(v^f)$:

$$
F(t_k + \tfrac{h}{2}) = L\bar{v}_{k+1}^f + N(\bar{v}_{k+1}^f). \tag{12}
$$

Deriving the stationarity conditions for (10) yields the following system of equations corresponding to the robot dynamics:

$$
\bar{q}_{k+1}^r - \tfrac{h}{2}\bar{v}_{k+1}^r = \bar{q}_k^r + \tfrac{h}{2}\bar{v}_k^r, \tag{13}
$$

$$
\begin{aligned}
M^r \bar{v}_{k+1}^r &+ h\big(\tfrac{\partial c_5}{\partial \bar{q}_k^r} + \tfrac{\partial c_5}{\partial \bar{q}_{k+1}^r}\big)^T \lambda_{5,k} \\
&+ \big(\tfrac{\partial c_6}{\partial v_k^r} + \tfrac{\partial c_6}{\partial v_{k+1}^r}\big)^T \lambda_{6,k} = M^r \bar{v}_k^r - hM^r g,
\end{aligned}
\tag{14}
$$

as well as that corresponding to the fluid dynamics:

$$
\begin{aligned}
\big(M^f - \mu \tfrac{h}{2} L\big)\bar{v}_{k+1}^f &- \tfrac{h}{2} N(\bar{v}_{k+1}^f) \\
&+ Gp_k + B\lambda_{3,k} + \big(\tfrac{\partial c_6}{\partial v_k^f} + \tfrac{\partial c_6}{\partial v_{k+1}^f}\big)^T \lambda_{6,k} \\
&= \big(M^f + \mu \tfrac{h}{2} L\big)\bar{v}_k^f + \tfrac{h}{2} N(\bar{v}_k^f) - hM^f g.
\end{aligned}
\tag{15}
$$

Finally, the constraints of (10) form the rest of the FON conditions, and the system of equations defined by (13)-(15) can be solved using Newton's method. Specifically, $\bar{q}_{k+1}^r, \bar{v}_{k+1}^r, \bar{v}_{k+1}^f$ and the corresponding dual variables can be solved for given $\bar{q}_k^r, \bar{v}_k^r, \bar{v}_k^f$. Upon further inspection, we note that this integration scheme is nearly equivalent to implicit Crank-Nicholson: a stable, energy-preserving Runge-Kutta method commonly used to integrate partial differential equations.

3 EXPERIMENTAL RESULTS

We validate our framework's ability to jointly simulate both robot and fluid dynamics. Specifically, we investigate the trajectory of a squid-like robot performing a hand-designed forward-swimming gait in an initially-still-water environment. An untethered, self-contained robot was designed and fabricated as shown in Figure 2a, and the 100×100-grid simulation environment is recreated in a real-world setup as shown in Figure 2b. The controls are defined as the angle between the robot fins at each timestep, ϕ_k.

As seen in Figure 3, our multiphysics approach is able to simulate the forward-swimming locomotion behavior, which is consistent with open-loop demonstrations on hardware. Specifically, our framework achieves an RMSE error of 0.89 cm over the whole trajectory. Meanwhile, Genesis [10], a state-of-the-art multiphysics simulator for robotics, has difficulty simulating the fluid-robot interaction to achieve forward motion, resulting in an RMSE error of 8.86 cm over which our framework improves by nearly 90%. We attribute this to Genesis's particle-based representation of the fluid [16, 25].

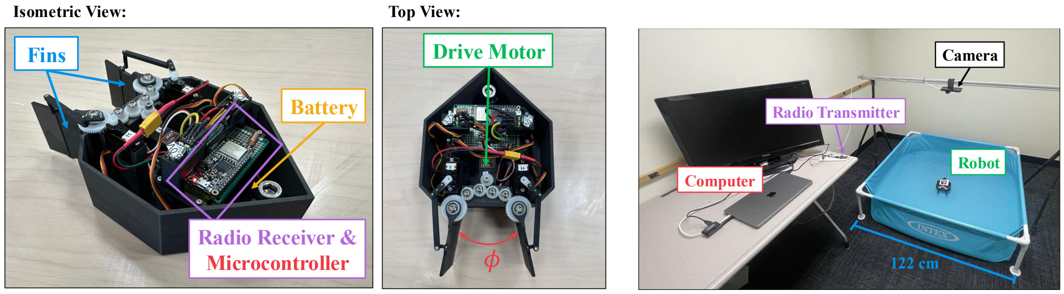

(a) Squid-like swimming robot hardware

(b) Hardware-experiment setup

Figure 2: Hardware-experiment setup for sim-to-real validation of a squid-like robot swimming in an initially-still-water environment. A real-world squid-like swimming robot is designed from the ground up to be untethered with an onboard battery, microcontroller, and radio transreceiver. The robot's servo motor drives the fins to the desired angle, ϕ. In this study, a computer sends motor commands over radio to the robot to execute an undulating, forward-swimming gait. The robot-configuration trajectory is tracked by a top-down-facing camera via an aruco marker.

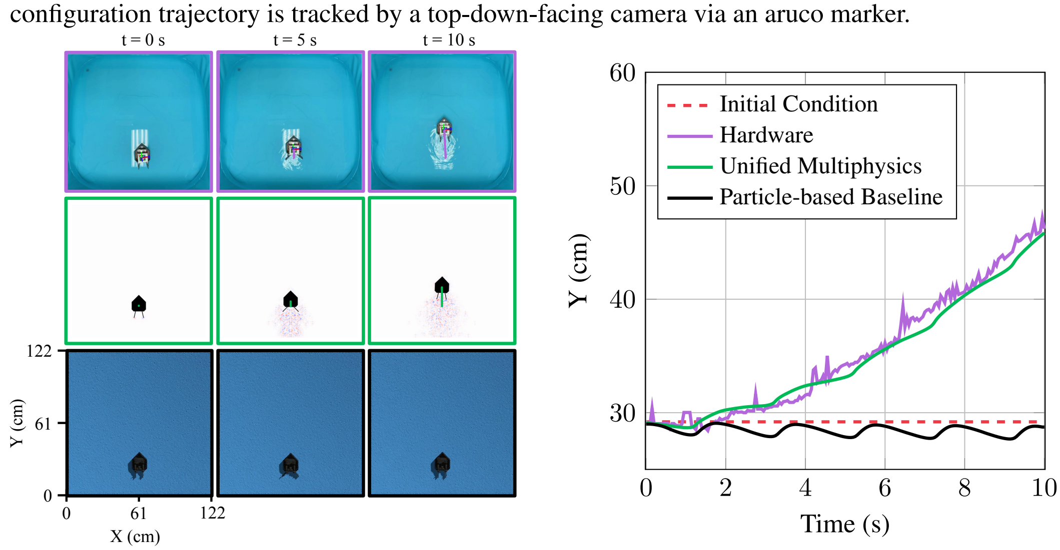

(a) Trajectory visualizations of the robot executing a forward-swimming gait. The top row shows the real robot, while the middle row is our method and the bottom row is a particle-based simulation.

(b) Time history of the robot position in the corresponding forward-swimming direction.

Figure 3: Sim-to-real validation of a squid-like robot executing an open-loop swimming gait in initially-still water. Our unified-multiphysics approach (green) is able to model the propulsion resulting from the fluid-robot interaction unlike the particle-based baseline in Genesis (black).

4 CONCLUSION

We have presented a unified framework for deriving and simulating fluid-robot multiphysics as a single optimization problem. Specifically, we model the unified least-action principle from which the coupled differential equations are derived. We build upon previous works in variational mechanics to discretize the action directly to simulate the fluid-robot interaction in a stable, tightly-coupled manner. The result is good agreement with real-world rollouts on a bioinspired robot.

In future work, we aim to address the current limitations of our variational method for downstream design and trajectory optimization tasks. We also hope to extend our framework to other non-rigid multiphysics problems commonly seen in robotics, such as deformable-object manipulation, rigid-soft robots that experience contact, etc.

References

[1] Z. Xu, C. Chi, B. Burchfiel, E. Cousineau, S. Feng, and S. Song. DextAIRity: Deformable Manipulation Can be a Breeze, 2022. URL https://arxiv.org/abs/2203.01197. _eprint: 2203.01197.

[2] H. Shi, H. Xu, S. Clarke, Y. Li, and J. Wu. Robocook: Long-horizon elasto-plastic object manipulation with diverse tools. *arXiv preprint arXiv:2306.14447*, 2023.

[3] U. Yoo, A. Hung, J. Francis, J. Oh, and J. Ichnowski. RoPotter: Toward Robotic Pottery and Deformable Object Manipulation with Structural Priors. In *2024 IEEE-RAS 23rd International Conference on Humanoid Robots (Humanoids)*, pages 843–850. IEEE, 2024.

[4] A. LaGrassa, M. Lee, and O. Kroemer. Task-Oriented Active Learning of Model Preconditions for Inaccurate Dynamics Models, 2024. URL https://arxiv.org/abs/2401.04007. _eprint: 2401.04007.

[5] J. Ichnowski, Y. Avigal, Y. Liu, and K. Goldberg. Gomp-fit: Grasp-optimized motion planning for fast inertial transport. In *2022 international conference on robotics and automation (ICRA)*, pages 5255–5261. IEEE, 2022.

[6] Z. Yang, M. N. Saadatzi, R. Zhang, A. Sherehiy, D. Wei, C. K. Harnett, and D. O. Popal. Multiphysics Dynamic Model Validation Methodology for Laser-Driven Microrobots. In *2019 IEEE 15th International Conference on Automation Science and Engineering (CASE)*, pages 1555–1561, 2019. doi:10.1109/COASE.2019.8843032.

[7] D. Costa, G. Palmieri, M.-C. Palpacelli, D. Scaradozzi, and M. Callegari. Design of a Carangiform Swimming Robot through a Multiphysics Simulation Environment. *Biomimetics (Basel, Switzerland)*, 5(4), Sept. 2020. ISSN 2313-7673. doi:10.3390/biomimetics5040046. Place: Switzerland.

[8] M. O'Connell, G. Shi, X. Shi, K. Azizzadenesheli, A. Anandkumar, Y. Yue, and S.-J. Chung. Neural-Fly enables rapid learning for agile flight in strong winds. *Science Robotics*, 7(66):eabm6597, 2022. doi:10.1126/scirobotics.abm6597. URL https://www.science.org/doi/abs/10.1126/scirobotics.abm6597. _eprint: https://www.science.org/doi/pdf/10.1126/scirobotics.abm6597.

[9] M. Macklin. Warp: A High-performance Python Framework for GPU Simulation and Graphics, Mar. 2022. URL https://github.com/nvidia/warp.

[10] G. Authors. Genesis: A Universal and Generative Physics Engine for Robotics and Beyond, Dec. 2024. URL https://github.com/Genesis-Embodied-AI/Genesis.

[11] J. M. Anderson and N. K. Chhabra. Maneuvering and stability performance of a robotic tuna. *Integrative and comparative biology*, 42(1):118–126, Feb. 2002. ISSN 1540-7063. doi:10.1093/icb/42.1.118.

[12] A. P. Maertens, A. Gao, and M. S. Triantafyllou. Optimal undulatory swimming for a single fish-like body and for a pair of interacting swimmers. *Journal of Fluid Mechanics*, 813:301–345, 2017. doi:10.1017/jfm.2016.845. Publisher: Cambridge University Press.

[13] A. Gao and M. S. Triantafyllou. Independent caudal fin actuation enables high energy extraction and control in two-dimensional fish-like group swimming. *Journal of Fluid Mechanics*, 850:304–335, 2018. doi:10.1017/jfm.2018.456. Publisher: Cambridge University Press.

[14] G. Novati, S. Verma, D. Alexeev, D. Rossinelli, W. M. Van Rees, and P. Koumoutsakos. Synchronisation through learning for two self-propelled swimmers. *Bioinspiration & biomimetics*, 12(3):036001, 2017. Publisher: IOP Publishing.

[15] R. K. Katzschmann, J. DelPreto, R. MacCurdy, and D. Rus. Exploration of underwater life with an acoustically controlled soft robotic fish. *Science Robotics*, 3(16):eaar3449, 2018. doi:10.1126/scirobotics.aar3449. URL `https://www.science.org/doi/abs/10.1126/scirobotics.aar3449`.

[16] J. G. Miles and N. A. Battista. Don't be jelly: Exploring effective jellyfish locomotion. *arXiv preprint arXiv:1904.09340*, 2019.

[17] Y. Jiao, F. Ling, S. Heydari, N. Heess, J. Merel, and E. Kanso. Learning to swim in potential flow. *Physical Review Fluids*, 6(5), May 2021. doi:10.1103/physrevfluids.6.050505. URL `https://doi.org/10.1103%2Fphysrevfluids.6.050505`. Publisher: American Physical Society (APS).

[18] J. Marsden and M. West. Discrete mechanics and variational integrators. *Acta Numerica*, pages 357–514, 2001.

[19] R. L. Seliger and G. B. Whitham. Variational principles in continuum mechanics. *Proceedings of the Royal Society of London. Series A. Mathematical and Physical Sciences*, 305(1480): 1–25, 1968. Publisher: The Royal Society London.

[20] V. I. Arnold and B. A. Khesin. *Topological methods in hydrodynamics*, volume 19. Springer, 2009.

[21] J. L. Lagrange. *Mécanique analytique*, volume 1. Mallet-Bachelier, 1853.

[22] J. H. Ferziger, M. Perić, and R. L. Street. *Computational methods for fluid dynamics*. springer, 2019.

[23] C. S. Peskin. The immersed boundary method. *Acta numerica*, 11:479–517, 2002.

[24] K. Taira and T. Colonius. The immersed boundary method: A projection approach. *Journal of Computational Physics*, 225(2):2118–2137, 2007. ISSN 0021-9991. doi:https://doi.org/10.1016/j.jcp.2007.03.005. URL `https://www.sciencedirect.com/science/article/pii/S0021999107001234`.

[25] Y. Hu, Y. Fang, Z. Ge, Z. Qu, Y. Zhu, A. Pradhana, and C. Jiang. A moving least squares material point method with displacement discontinuity and two-way rigid body coupling. *ACM Transactions on Graphics (TOG)*, 37(4):1–14, 2018. Publisher: ACM New York, NY, USA.